

# Self-compacting concrete using calcium-rich ashes as alternative fillers and heated dry materials to simulate hot weather mixing

*Concretos autoadensáveis com cinzas ricas em cálcio como filer alternativo e materiais secos aquecidos para simular mistura sob clima quente*

Jonatércio Florêncio de Vasconcelos Marinho 

Rodrigo Araújo Pereira Lima 

Erika Pinto Marinho 

Ana Cecilia Vieira da Nóbrega 

## Abstract

**A**lgaroba wood (*Prosopis juliflora*) is commonly used as energy source in the northeast region of Brazil and India, generating rich-calcium carbonate ( $\text{CaCO}_3$ ) ashes as a promising alternative limestone filler. Moreover, concreting in hot climates (for example, in tropical regions) can affect its fresh state conditions owing to the evaporation of the mixing water. Thus, Self-Compacting Concretes (SCCs) incorporating Algaroba ashes were produced using heated dry materials ( $80 \pm 2^\circ\text{C}$ ) to simulate hot weather mixing (on site,  $50 \pm 2^\circ\text{C}$ ). In order to simulate the hot weather conditions on site for subsequent control tests over time (in the laboratory), the specimens were cured in water at  $20 \pm 2^\circ\text{C}$ . The self-compacting ability at the end of mixing was kept constant by extra water addition or superplasticizer overdosing. The partial replacement of 50% of natural lime filler by calcium-rich ash preserved the compressive strength and permeability of mixtures with 100% of limestone filler. Using 50% ash also demanded less water and superplasticizer when submitted to the simulated hot weather mixing.

**Keywords:** Self-compacting concrete. Algaroba tree ashes. Hot weather.

## Resumo

*A madeira de Algaroba (Prosopis juliflora) é comumente usada na região nordeste do Brasil e na Índia como matriz energética, gerando cinzas ricas em carbonato de cálcio ( $\text{CaCO}_3$ ), promissores fileres calcários alternativos. Adicionalmente, concretar em climas quentes (por exemplo, em regiões tropicais) pode afetar o estado fresco devido à evaporação da água de mistura. Concretos Auto Adensáveis (CAAs) incorporando cinzas de Algaroba foram produzidos usando materiais secos aquecidos ( $80 \pm 2^\circ\text{C}$ ) para simular mistura sob clima quente (em obra,  $50 \pm 2^\circ\text{C}$ ). A fim de simular as condições de clima quente em obra para posterior teste de controle ao longo do tempo (em laboratório), as amostras foram curadas em água a  $20 \pm 2^\circ\text{C}$ . A auto-adensabilidade foi mantida constante ao final das misturas pela adição de água extra ou superdosagem de superplastificante. A substituição parcial de 50% do filer calcário por cinzas ricas em cálcio preservou a resistências à compressão e permeabilidade das misturas com 100% de filer calcário. O uso de 50% de cinza também demandou menos água e superplastificante em condição simulada de mistura sob clima quente.*

**Palavras-chave:** Concreto autoadensável. Cinzas de Algaroba. Clima quente.

<sup>1</sup>Jonatércio Florencio de Vasconcelos Marinho

<sup>1</sup>Universidade Federal de Pernambuco  
Caruaru - PE - Brasil

<sup>2</sup>Rodrigo Araújo Pereira Lima

<sup>2</sup>Universidade Federal de Pernambuco  
Caruaru - PE - Brasil

<sup>3</sup>Erika Pinto Marinho

<sup>3</sup>Universidade Federal de Pernambuco  
Caruaru - PE - Brasil

<sup>4</sup>Ana Cecilia Vieira da Nóbrega

<sup>4</sup>Universidade Federal do Rio Grande do Norte  
Natal - RN - Brasil

Recebido em 04/07/21

Aceito em 12/09/22

## Introduction

The tropical climate is predominant in Brazil's northeast region, and the influence of the temperature inherent to this climate is usually ignored in construction. Concreting in hot climates can impair the properties of cement systems, being deleterious for the transporting, placing and consolidation of concrete (MASSARWEH *et al.*, 2020; GHAFoori; DIAWARA; HASNAT, 2018). Pineaud *et al.* (2016) and Nóbrega *et al.* (2018) highlighted that the effects of temperature in Self Compacting Concretes (SCCs) have been little studied and, through tests, found that this factor interferes with the mechanical properties of SCC.

According to ACI 305.1 (AMERICAN CONCRETE..., 2014), the water consumption increases significantly when the initial temperature of the concrete made from ordinary Portland cement reaches 30 °C. Prior studies have proved that the main consequences of the influence of hot weather on ordinary vibrated concrete are as follows: high temperature during mixing and curing, with a maximum value of 50 °C; loss of workability and increased water consumption (HAMPTON, 1981; MOURET; BASCOUL; ESCADEILLAS, 2003); and, although the compression strength has increased at early ages (MOURET; BASCOUL; ESCADEILLAS, 2005; ORTIZ *et al.*, 2005), losses in this parameter are reported at 28 days of age or more (KANSTAD *et al.*, 2003; MOURET; BASCOUL; ESCADEILLAS, 2005; ORTIZ *et al.*, 2005; MASSARWEH *et al.*, 2020). Zhang, Li and Li (1999) observed a decrease in compressive strength at 28 days when the concrete temperature during the first 24 h was 38 °C.

On the other hand, Nóbrega *et al.* (2018) found a behavior in SCC different from that in ordinary vibrated concrete with respect to the development of compressive strength. However, they found that concrete mixed at approximately 50 °C required correction with water or superplasticizer to maintain its self-compacting properties. SCCs mixed and/or cured under elevated temperatures showed compressive strength results that not only increased at 1 day of age but were unchanged or increased at 7 and 28 days, regardless of the means used to maintain the self-compacting ability constant. Corrections using superplasticizer should be preferred in this case because this water correction can have a negative influence when compared to the superplasticizer one, leading to decreased compressive strength, durability, passing ability, flowability, and plastic viscosity.

This performance is different between the SCC and the usual vibrated concrete despite the materials of identical bases and nature (cement), due to the high demand of fines and superplasticizer by the SCC. The difference in mixture composition changes not only the morphology and density of the C-S-H formed, but also interferes in the quality of the transition zone between the cementitious matrix and the gravel. Hence, SCCs seem to be promising for use in hot weather conditions when compared to the ordinary vibrated concrete.

To add water in the concrete was a common practice to overcome the water evaporation due to mix and cast concretes under hot weather conditions, which can be also counteracted using superplasticizers (NÓBREGA *et al.* 2018; RAHAL; HASSAN, 2021; MASSARWEH *et al.*, 2020; GHAFoori; DIAWARA; HASNAT, 2018). For instance, very high water to cement ratios were used in the past in Kuwait to achieve adequate slump suitable for concreting in the local hot weather condition with a consequent low-strength concrete (RAHAL; HASSAN, 2021). Ghafoori *et al.* (2018) proposed to remediate the loss in flow properties of self-consolidating concrete under hot temperatures using superplasticizer, where its overdosing increased with increases in both hauling time and temperature (GHAFoori *et al.*, 2018).

Another observation about preparing (mixing and casting) concretes under hot weather conditions (on site) is related to the subsequent control tests over time (in the laboratory). The samples are prepared on site and afterwards underwater cured on site before the age of the tests, or immediately transported to the laboratory for further analysis. In both of these cases, the samples are cured at environmental temperature. Although these control sample cure conditions are different from the concrete cured on site under hot weather conditions, they are the ones used as control specimens to the testing laboratory, which implies the acceptance or rejection of that already placed concrete (NÓBREGA *et al.*, 2018). Hence, this work simulates the evaluation of these control samples of the SCCs that have just been prepared (mixing and casting) under hot weather conditions, not addressing the on-site hot weather curing.

It is also known that the use of fines (fillers), combined with the use of a superplasticizer, allows SCC to have good rheological and non-segregation properties (TUTIKIAN; DAL MOLIN, 2008; BRADU; FLOREA, 2015). Furthermore, recent research indicates that the limestone fillers also have reactivity, with the formation of carboaluminates and monocarboaluminates, which positively influence the microstructures of cementitious materials (MOON *et al.*, 2017; SCHÖLER *et al.*, 2017).

As the limestone filler is a non-renewable source, the possibility of using calcium-rich ash is evaluated because it is composed mainly of calcium carbonate (around 70% – 80%  $\text{CaCO}_3$ ) without expansive oxides (LELOUP, 2013; NASCIMENTO, 2014; NASCIMENTO *et al.*, 2019; MOURA *et al.*, 2021; MELO *et al.*, 2018). The size of Algaroba wood ash grains that pass through sieve no. 200 is between 2.46  $\mu\text{m}$  and 43.91  $\mu\text{m}$  (NASCIMENTO *et al.*, 2019; MELO *et al.*, 2018), which is within the grain size required to use as a filler in SCC systems. Thus, owing to the similarity of this type of ash with the natural limestone filler regarding its chemical composition and possible treatments in the physical aspect, it is observed that SCC can incorporate calcium-rich ashes as an alternative filler to ensure its fluidity. According to Lima, Marinho and Nóbrega (2019), the substitution of the limestone filler with calcium-rich ash is viable in a proportion of up to 50%, providing improvements in the durability and strength of concrete in the first ages, reaching 31 MPa at 28 days.

The introduced *Prosopis Juliflora* tree is use as biomass for energy generation is allowed by Law No. 12651/2012 of the new Brazilian Forest Code (MOURA *et al.*, 2021). In this context, Algaroba wood is the fuel used by approximately 240 laundries in the Agreste Pernambucano region of Brazil (MOURA, 2017; MOURA *et al.*, 2021). In a medium-sized laundry, the waste generated by the burning of Algaroba wood is approximately 6,500 kg/month of ash (MELO, 2012; MOURA *et al.*, 2021). In some cases, these ashes are used for soil pH correction, but most of the residue is still discarded in the environment without any control or criteria (MOTA, 2014).

Therefore, considering the environmental conditions in this tropical region, this research aims to evaluate the effects of mixing and casting temperatures in SCCs samples produced on site ( $50 \pm 2$  °C) using heated dry materials ( $80 \pm 2$  °C) for further control tests over time in the laboratory ( $20 \pm 2$  °C). The incorporation of calcium-rich ash as an alternative to the limestone filler was also considered as an environmental approach.

## Experimental program

### Materials

#### Cement

CPV-ARI cement was used according to the technical bulletin provided by the supplier, and its physical and chemical properties are listed in Table 1. The chemical characterization was performed by X-ray fluorescence using a Rigaku spectrometer (Primini model) with 50 W tube tension (Na to U) and pressed samples.

Table 1 - Physical and chemical properties of CPV-ARI cement

Determination		CPV-ARI	
Physical properties	Composition	Clinker	98.50%
		Limestone	0 a 10%
	Density	$\text{g/cm}^3$	3.09
	Fineness	Residue at 75 $\mu\text{m}$ (%)	$\leq 0.22$
		Blaine ( $\text{cm}^2/\text{g}$ )	$\geq 4.692$
	Setting time	Initial (min)	$\geq 95$
		Final (min)	$\leq 180$
	Expansibility	In hot conditions (mm)	$\leq 2$
	Compressive strength	1 day (MPa)	$\geq 17.48$
		3 days (MPa)	$\geq 27.00$
7 days (MPa)		$\geq 36.00$	
Chemical composition	Insoluble residue (%)	$\leq 1.00$	
	LOI (%)	$\leq 4.37$	
	$\text{SiO}_2$ (%)	20.43	
	$\text{Al}_2\text{O}_3$ (%)	4.90	
	$\text{Fe}_2\text{O}_3$ (%)	1.83	
	CaO (%)	65.40	
	$\text{SO}_3$ (%)	3.60	
	MgO (%)	1.06	
$\text{K}_2\text{O}$ (%)	0.27		

Source: physical properties from a technical bulletin provided by the supplier.

## Limestone filler and calcium-rich ashes

The limestone filler used was of calcitic sedimentary origin with a dimension of less than 0.075 mm, corresponding to the No. 200 sieve.

The Algaroba wood (*Prosopis juliflora*) ash was collected in a laundry in Caruaru/PE, which uses this wood as the only fuel in its kilns. After collection, the ashes were dried in an oven at 105 °C, sieved in a 4.75 mm mesh to remove larger particles, and finally sieved through a No. 200 sieve.

The filler and the calcium-rich ashes were then characterized by X-ray fluorescence using a Rigaku spectrometer, Primini model, with tube tension of 50 W (Na to U), and pressed samples, and by X-ray diffraction using a Bruker D8 Advanced Davinci diffractometer, with radiation CuK $\alpha$  (40 kV / 40 mA), and with a 0.02° step every 0.5 s in the interval 5° < 2 $\theta$  < 70°. The physicochemical properties of the limestone filler and calcium-rich ashes are presented in Table 2.

The X-ray diffraction analyses of the limestone filler (Figure 1a) and calcium-rich ashes (Figure 1b) indicate in both cases calcium carbonate (CaCO<sub>3</sub>) as the peak of greater intensity, near 30°. The microscopic study of the calcium-rich ashes was performed using a SSX-500 Shimadzu scanning electron microscope. The samples were fixed with carbon tape after passing through a gold metallization for 5 min with a potential variation of 1.8 kV (LELOUP, 2013).

The thermogravimetric analysis (TGA) of the calcium-rich ash showed the major presence of CaCO<sub>3</sub> with a loss of mass (31.07%) at the peak of 800 °C due to its decomposition (Figure 2).

Table 2 - Chemical and physical properties of limestone fillers and calcium-rich ashes

Chemical composition								
Oxides (%)	MgO	Al <sub>2</sub> O <sub>3</sub>	SiO <sub>2</sub>	P <sub>2</sub> O <sub>5</sub>	Fe <sub>2</sub> O <sub>3</sub>	SO <sub>3</sub>	K <sub>2</sub> O	CaO
Limestone filler	5.11	1.49	3.23	0.22	1.9	0.12	0.28	87.65
Calcium-rich ashes	2.44	0.37	0.83	1.99	0.35	1.33	12.30	77.52
Physical properties								
Fineness/ratio	Limestone filler		Calcium-rich ashes					
Blaine (cm <sup>2</sup> /g)	5.096		6.857					
BET (cm <sup>2</sup> /g)	30,045		47,142					
Bulk density (g/cm <sup>3</sup> )	2.71		2.76					
CaO/SiO <sub>2</sub>	27.13		93.40					
SiO <sub>2</sub> /CaO	0.037		0.010					
MgO/SiO <sub>2</sub>	1.58		2.93					

Figure 1 - X-ray diffractogram of limestone filler (a) and calcium-rich ashes (b)

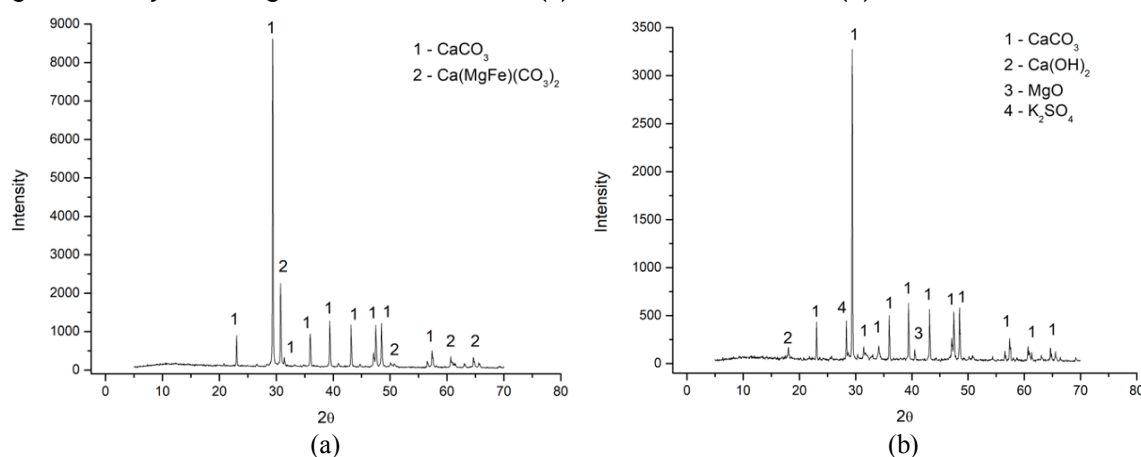
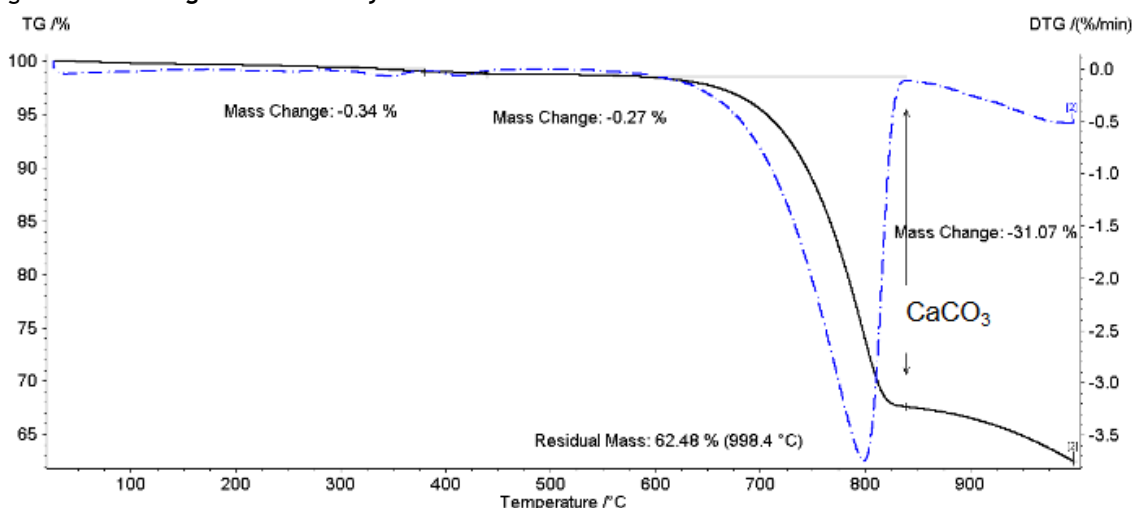


Figure 2 - Thermogravimetric analysis of calcium-rich ashes



### Aggregates

Granite aggregate with a specific mass of 2.63 g/cm<sup>3</sup>, bulk density of 1.36 g/cm<sup>3</sup>, and maximum diameter of 9.5 mm was used as gravel, and the siliceous sand had a maximum size of 4.75 mm, bulk density of 2.58 g/cm<sup>3</sup>, and unit mass of 1.47 g/cm<sup>3</sup>. Based on the large and small aggregates, an optimized compact granular skeleton of silicone–granite (1:1) was developed with a diameter of 0–9.5 mm, unit mass of 1.415 g/cm<sup>3</sup>, and bulk density of 2.605 g/cm<sup>3</sup>. All aggregates were dried in an oven at 105 °C prior to use. The granulometric distributions of the aggregates and Granular Skeleton (GS) are shown in Figure 3.

The aggregate reactivities for both sand and gravel were assessed through the determination of the expansion in mortar bars using the accelerated method according to that presented by NBR 15577-4 (ABNT, 2018a) which is based on the American standard C 1260 (AMERICAN SOCIETY..., 2014b) and the Canadian CSA A23.2-25A (CANADIAN..., 2014). As shown in Figure 4, the used sand was potentially reactive, unlike the gravel, which was potentially innocuous.

As the small aggregate was potentially reactive, the maximum content of the substitution of limestone filler with calcium-rich ash is 26%, obeying the tolerance of 0.60% of alkaline equivalent sodium concentration (%Na<sub>2</sub>O<sub>eq</sub> = %Na<sub>2</sub>O + 0.658 %K<sub>2</sub>O (ABNT, 2018b)), as established by C 150 (AMERICAN SOCIETY..., 2017a) and C 227 (AMERICAN SOCIETY..., 2010). In the latter case, considering a 25% addition in relation to the cement's weight, it would only be admissible to add up to 6.5% of Algaroba ash to inhibit such a reaction. However, because this study focuses on verifying the incorporation of Algaroba ash that provides the SCC with the best result, this limitation was not considered. This verification was only performed to alert and register the possible risk of such an occurrence. Non-reactive aggregates, the use of mitigating additions, or limiting the content of limestone addition in SCC production are interesting choices for inhibiting the alkali-aggregate reaction.

### Liquids

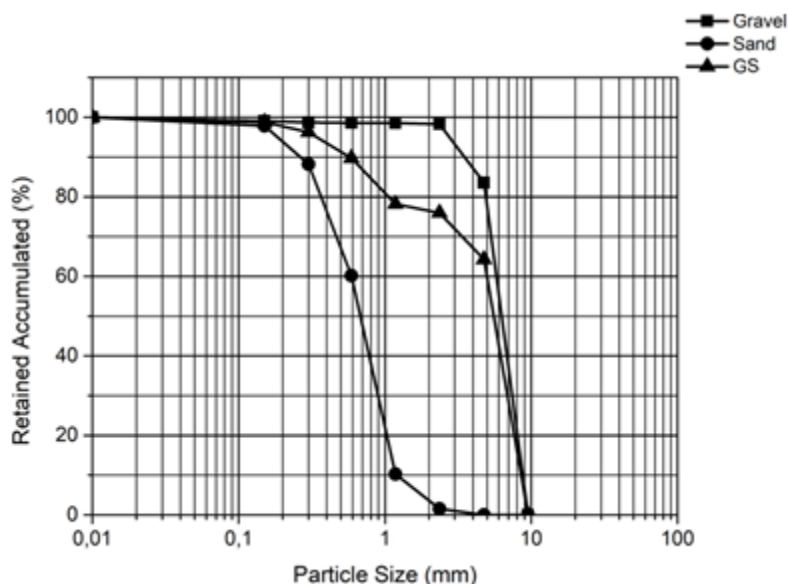
Glenium 51–BASF was used as a superplasticizer. It is based on a modified polycarboxylic ether chain, with a density of 1.067–1.107 g/cm<sup>3</sup>, active solid content by weight of 28.5%, viscosity < 150, and pH = 5–7. Finally, distilled water with a pH of 6.55 was used.

### Design of SCCs

Table 3 presents the material consumption (kg/m<sup>3</sup>) and the nomenclature used for each mixture, being named TFC (100% of limestone filler), TFCFA (50% of limestone filler + 50% of calcium-rich ash filler), and TFA (100% of calcium-rich ash filler) mixed and cured at 20 ± 2 °C. As shown in Table 3, the total fine (cement and limestone filler) consumption was 450 kg/m<sup>3</sup>, with 360 kg/m<sup>3</sup> of cement and 90 kg/m<sup>3</sup> of limestone filler or calcium-rich ash. The water/total fines ratio adopted was 0.50, and the content of superplasticizer was adjusted to obtain a spread between 660 and 750 mm, class SF2 according to NBR 15823-1 (ABNT, 2017a). The optimized compact granular skeleton of silicone–granite (1:1) was used. Finally, an air void content of 25 L/m<sup>3</sup> in concrete was considered to calculate the consumption of materials (NÓBREGA *et al.*, 2018). The choice of these proportions was based on the study by Lima, Marinho and

Nóbrega (2019), where the mixture with 50% substitution of limestone filler with calcium-rich ashes presented better behaviors for the fresh and hardened states. Although the result of 100% substitution was not promising, it was chosen to observe its performance under hot weather conditions.

Figure 3 - Granulometric curves of the gravel, sand optimized granular skeleton (GS)



## Design of SCCs using heated dry materials to simulate hot weather mixing

To simulate the preparation of the SCC specimens under hot weather conditions (on site) for subsequent control tests over time (in the laboratory), the raw materials were preheated in an oven up to  $80 \pm 2$  °C, and the specimens were cured in water at  $20 \pm 2$  °C. The temperature values of cement, filler, and aggregates were raised to  $80 \pm 2$  °C to maintain the temperature at the end of the mixture around  $50 \pm 2$  °C (NÓBREGA *et al.*, 2018). Water and superplasticizer were kept at  $20 \pm 2$  °C, which is an acceptable value for distribution and storage conditions. SCC mixtures mixed and cast at  $20 \pm 2$  °C were used as reference.

A temperature close to reality was determined in the field to evaluate the properties of SCC mixed and cast under hot weather conditions. The temperatures of materials exposed to solar incidence were measured using an infrared thermometer at approximately 1 PM (13:00) on alternate days and weeks. When exposed to solar incidence in a tropical climate region in summer, it was verified that aggregates and cement could easily reach temperatures above 70 °C. Cement trucks that feed silos often remain hot in concrete plants and are used at temperatures above 70 °C.

Hence, to maintain the slump-flow spread between 660 mm and 750 mm (class SF2 (ABNT, 2017a)) due to the water evaporation imposed by the temperature during mixing and casting in hot weather conditions, two different types of correction were evaluated: water increment (TFC-W, TFCFA-W, and TFA-W mixed and cured at  $50 \pm 2$  °C) and superplasticizer increment (TFC-S, TFCFA-S, and TFA-S mixed and cured at  $50 \pm 2$  °C), as proposed by Nóbrega *et al.* (2018). Table 4 also lists the total volumes of water and superplasticizer, properly adjusted to the maintenance of the slump-flow spread in hot weather conditions. Nóbrega *et al.* (2018) did not observe significant increases in the actual water content measured at the end of the mixing in SCCs, considering the accuracy of  $\pm 3$  kg/m<sup>3</sup>, whatever the means employed to keep the self-compacting ability constant (by adding extra water or overdosing superplasticizer). Hence, it was assumed that all evaporated water was exactly replaced by the extra water added, remaining the consumption of dry materials unchanged.

### Mixing procedure

The mixing was carried out in an air-conditioned room ( $20 \pm 2$  °C) in a stationary shaft concrete mixer with a capacity of 120 L. Regarding the mixed and cast mixtures at  $20 \pm 2$  °C, all materials were placed in hermetically sealed containers in an air-conditioned room ( $20 \pm 2$  °C) for about 4 hours. In the case of the mixing at  $50 \pm 2$  °C, all materials previously heated to  $80 \pm 2$  °C (24h) were removed from the oven immediately before use. The gravel, fillers, cement, and sand were mixed for 60 s. In the sequence, all the water and 1/3 of the superplasticizer were added and mixed for 90 s. Finally, the rest of the superplasticizer was added and mixed for another 90 s. For the temperature of  $50 \pm 2$  °C, water or superplasticizer increments were added in steps of 30 s, not exceeding the limit time of 5 min of total mixing (NÓBREGA *et al.*, 2018). If this time was exceeded, the sample was discarded.

Table 4 - Composition and nomenclature of the SCCs designs using heated dry materials to simulate hot weather mixing

Nomenclature	T <sub>mc</sub> (°C)	Cement (kg/m <sup>3</sup> )	Limestone filler (kg/m <sup>3</sup> )	Calcium-rich ash (kg/m <sup>3</sup> )	Gravel (kg/m <sup>3</sup> )	Sand (kg/m <sup>3</sup> )	Total water (kg/m <sup>3</sup> )	Actual water (kg/m <sup>3</sup> )	SP (% BWOC <sup>**</sup> )	Slump (mm)
TFC-W	50	360	90	-	784.69	784.69	265	225	0.4375	660
TFC-S	50	360	90	-	784.69	784.69	225	225	0.7775	700
TFCFA-W	50	360	45	45	785.08	785.08	238	225	0.9375	685
TFCFA-S	50	360	45	45	785.08	785.08	225	225	1.005	665
TFA-W	50	360	-	90	785.47	785.47	265	225	1.125	670
TFA-S <sup>***</sup>	50	360	-	90	785.47	785.47	225	225	-	-

Note: \*T<sub>mc</sub> = approximately mixing and casting temperature; \*\*BWOC = by weight of cement; and \*\*\*it was not possible to produce a SCC of class SF2 for TFA-S. It was tested up to 2.078 (% BWOC) of superplasticizer.

The temperatures of the SCC mixtures during mixing were monitored using an infrared thermometer, and the average temperature curve for the SCCs is shown in Figure 5. In both cases, the average temperature of approximately 50 °C, expected at the end of the mixture, is highlighted. Samples of 10 cm × 20 cm (diameter × height) were molded according to NBR 5738 (ABNT, 2015). After 24 h, all the samples were demolded and immersed in water at room temperature ( $20 \pm 2$  °C) until the tests were performed. The cure was performed for all specimens at  $20 \pm 2$  °C.

## Methods

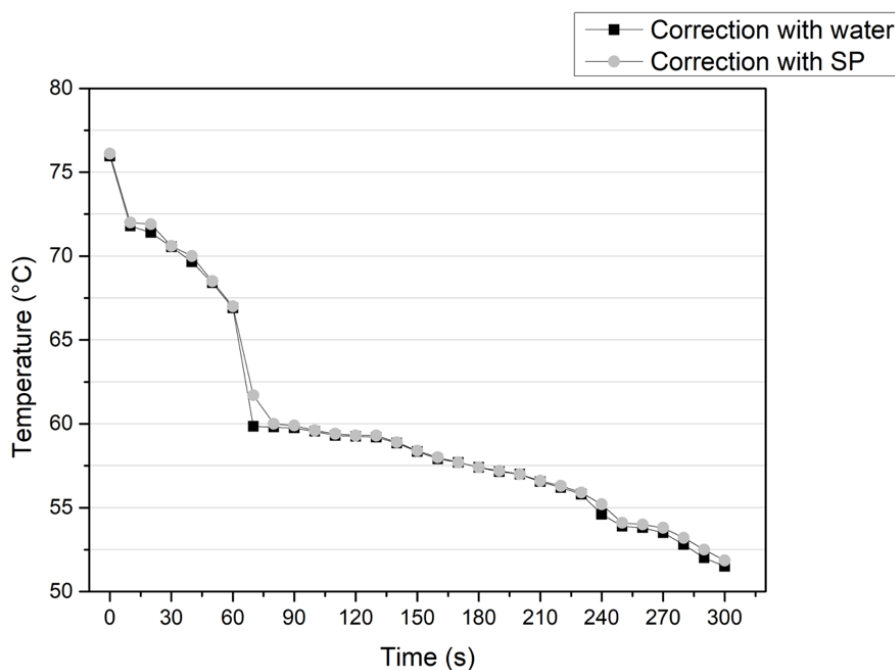
The behavior of the produced SCCs was evaluated using the following tests: slump flow (ABNT, 2017b),  $t_{500}$  (ABNT, 2017b), J-ring (ABNT, 2017e), L-Box (ABNT, 2017c), V-funnel (ABNT, 2017d), and segregation through the Visual Stability Index (VSI) (ABNT, 2017b).

The compression strength was evaluated at 1, 7, and 28 days (ABNT, 2018c). A Shimadzu brand press (model UH-2000KN) with a load cell capacity of 200 tons was used. Bar plot shows mean Coefficients of Variation (CV) of five samples for each mixture. At 28 days, the total absorption (ABNT, 2009), capillary absorption (ABNT, 2012), acid attack (acetic, sulfuric, hydrochloric), and electrical resistivity (LAVAGNA *et al.*, 2018) were measured in triplicate for each mixture, joining the standard deviation analysis to the results.

Three types of acids – acetic acid ( $\text{CH}_3\text{COOH}$ , 0.1 M), hydrochloric acid (HCl, 0.1 M), and sulfuric acid ( $\text{H}_2\text{SO}_4$ , 0.1 M) – were used for the acid attack test. The samples were extracted from the core of the concrete sample ( $2 \times 2 \times 2$  cm), dried in an oven ( $65 \pm 5$  °C, 48 h), weighed, and then immersed in a 1 L container containing 500 mL of each acid. The containers were agitated at 30 rpm for 24 h, according to NBR 10005 (ABNT, 2004). The final masses of the samples were measured after drying in an oven at  $65 \pm 5$  °C for 48 h; then, they were compared to the initial masses. The results are expressed as percentages followed by their standard deviation values.

The electrical resistivity was measured by applying an alternating current of 300 mV at 200 kHz in samples dried in an oven (105 °C, 24 h) with dimensions of 10 cm × 10 cm (diameter × height) in triplicate for each mixture. The test was performed by fixing two electrodes on the copper plates at the ends of the cylindrical samples. A water-dampened sponge was used as a conductor to improve the electrical contact between the electrodes and the sample.

Figure 5 - Temperature as a function of time during mixing



## Results and discussion

### Maintenance of the slump-flow spread in hot weather conditions

Table 5 lists the results of the tests in the fresh state of the proposed mixtures, including the slump flow,  $t_{500}$ , L-Box, J-Ring, V-Funnel, and VSI, according to the NBR 15823-1 (ABNT, 2017a) standard. The total volumes of water and superplasticizer properly adjusted for the corrections of the mixture spread in hot weather conditions are again presented for the sake of clarity.

As shown in Table 5, when the correction of the mixture spread under hot weather conditions was performed by adding water, there was a higher water demand of approximately 18% for the standard mixture (TFC, 100% of limestone filler) and in the case of total substitution of limestone filler with calcium-rich ashes (TFA, 100% of calcium-rich ashes). For a partial substitution (50%) of limestone filler with calcium-rich ashes (TFCFA), the extra water demand was reduced to 6%. Similar behavior was observed by Nóbrega *et al.* (2018).

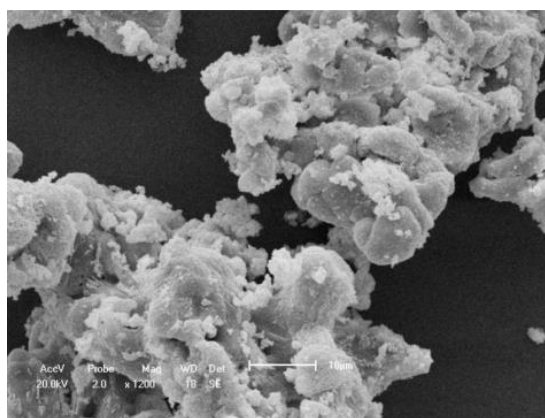
The low water demand in the partial substitution of limestone filler with calcium-rich ash is favorable for microstructural development. This is due to the low water loss by evaporation and is closely related to the morphology of the calcium-rich ash particles, as it can be observed in the micrographs (Figure 6). Despite having a larger specific surface area, the calcium-rich ashes do not demand more water in the TFCFA mixture, probably because of the agglomeration process or due to a better granular packing between the ashes and the limestone filler. Hence, the higher compactness of the system decreases the evaporation of the mixing water, and consequently the consumption of extra water and SP to maintain the workability. Furthermore, it is believed that their irregular and porous appearance in the agglomerations facilitated the trapping of water, avoiding its evaporation in hot climates.

Table 5 - Fresh state results and their respective classifications

Nomenclature	Slump (mm)	$t_{500}$ (s)	L-Box (mm/mm)	J-Ring (mm)	V-Funnel (s)	Classification (ABNT, 2017a)
TFC	700	1.6	0.92	15	4.5	SF2, VS1, PJ1, VF1, IEV 1
TFC-W	660	1.8	0.85	50	4.3	SF2, VS1, PJ2, VF1, IEV 0
TFC-S	700	2.0	0.71	20	5.1	SF2, VS1, -, VF1, IEV 1
TFCFA	665	1.3	0.81	22	5.2	SF2, VS1, PJ1, VF1, IEV 0
TFCFA-W	685	1.5	0.83	30	3.0	SF2, VS1, PJ2, VF1, IEV 1
TFCFA-S	665	1.7	0.80	24	6.0	SF2, VS1, PJ1, VF1, IEV 0
TFA	695	2.3	0.76	15	6.8	SF2, VS2, -, VF1, IEV 1
TFA-W	670	1.0	0.82	45	2.5	SF2, VS1, PJ2, VF1, IEV 0
TFA-S*	-	-	-	-	-	-

Note: \*it was not possible to produce a SCC of class SF2 for TFA-S. Up to 7.480 kg/m<sup>3</sup> of superplasticizer was tested.

Figure 6 - Micrography by SEM of the calcium-rich ash



In addition, the accommodation between the materials and their physicochemical characteristics can facilitate or hinder the dissipation of temperature, influencing the evaporation of water and/or interaction with the superplasticizer during the mixing process.

The demand for superplasticizer increased for higher calcium-rich ash contents for both SCC mixtures at  $20 \pm 2$  °C and at  $50 \pm 2$  °C. This behavior was due to the progressive increase in the specific surface area of the fines because these ashes have a specific BET area of 47,142 cm<sup>2</sup>/g against the 30,045 cm<sup>2</sup>/g of the limestone filler. When the correction of the spread of the mixture under hot weather conditions was performed by adding a superplasticizer, it had a higher demand, of approximately 78% for the standard mixture (TFC, 100% of limestone filler). The extra demand of superplasticizer was reduced to 6% when the limestone filler was partially substituted (50%) with calcium-rich ashes (TFCFA).

When correcting the mixture with superplasticizer in hot weather conditions, it was observed that the calcium-rich ashes demanded fewer additives than the natural limestone filler when compared with the reference mixture ( $20 \pm 2$  °C). The increase in the superplasticizer necessary in these environmental conditions is due to the increase in the specific surface area of the calcium-rich ashes. However, the morphology of the ash resulted in less evaporation of water during mixing. It is also important to note that the dispersion of cement particles increases with the amount of superplasticizer. Thus, the cement dispersion was improved in mixtures with calcium-rich ashes.

Finally, it is essential to note that it was impossible to produce a SCC of class SF2 when there is a total substitution of limestone filler with calcium-rich ashes (TFA, 100% of calcium-rich ashes), even with the insertion of up to 7,480 kg/m<sup>3</sup> of superplasticizer. It is believed that there is a possible interaction between the calcium-rich ashes and the chemical additive, which also has the undesirable effect of fast hardening of the mixture.

According to Table 4, the properties of fluidity, flow, passing ability, and resistance to segregation were achieved for the standard mixture (TFC, 100% of limestone filler), obtaining SCCs with classes SF2, VS1, PJ1, and VF1 (ABNT, 2017a). For the partial substitution of limestone filler (50%) with calcium-rich ashes (TFCFA), the same classes were obtained. However, in the case of total substitution of the limestone filler with calcium-rich ashes (TFA, 100% of calcium-rich ashes), there was a loss in the passing ability in a confined flow (L-Box), but still it met the free flow test (J-Ring).

Under hot weather mixing conditions, the standard mixture (TFC, 100% lime filler) reached all the self-compacting properties when corrected with the addition of water. However, when corrected with the addition of a superplasticizer, it did not meet the passing ability test in a confined flow (L-Box). For the partial substitution of limestone filler (50%) with calcium-rich ashes (TFCFA), the same classes of the standard mixture at  $20 \pm 2$  °C were also met, regardless of whether the correction was performed with the addition of water or superplasticizer, except in terms of classes PJ1 and PJ2, but both were acceptable. By replacing 100% lime mortar with the alternative mortar, although it was not possible to produce a SCC of class SF2 (tested up to 7,480 kg/m<sup>3</sup> of superplasticizer), correction with water was possible, leading to the same classification as that of the standard mixture at  $20 \pm 2$  °C.

The results show that water corrections improve the flow in confined flow tests (Funnel-V) and act inversely in a free flow ( $t_{500}$ ). It was also found that TFCFA, TFCFA-W, and TFCFA-S decreased the flow, indicating a positive effect of calcium-rich ashes, both for the reference mixture and for the mixture under hot weather conditions. Finally, it was verified that for TFA-W, the calcium-rich ashes acted positively with respect to the temperature effects, decreasing the flow values and improving the ability to pass in a confined flow.

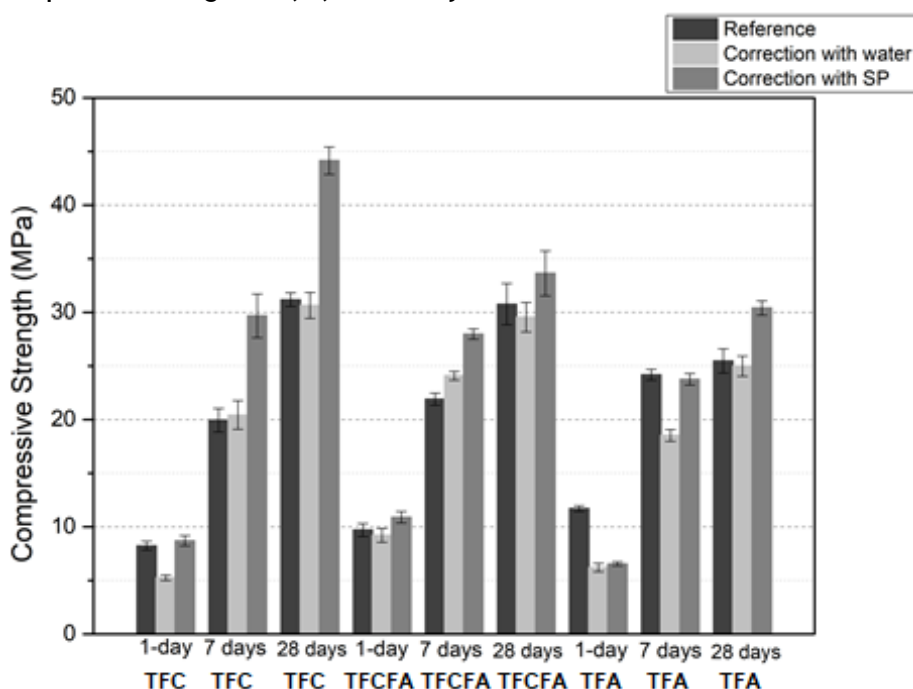
## Hardened state responses

### Compressive strength

The compressive strength values measured at 1, 7, and 28 days of age are shown in Figure 7. Bar plot shows mean Coefficients of Variation (CV).

In all systems, the correction with a superplasticizer to minimize the effects of water evaporation associated with the accelerated kinetics of ionic dissolution and hydration reactions during mixing in hot weather conditions was more promising for compression strength. There was a coefficient of variation between 1.70% (1 day) and 6.0% (7 days) for the compression strength specimens.

Figure 7 - Compression strength at 1, 7, and 28 days



Although at 1 day the gain in strength was slower in hot weather conditions and using water addition, the correction with water still maintained the levels of compression strength of the reference SCC, mainly at 28 days. For the system with 100% limestone filler (TFC), an average increase in compression strength of approximately 10 and 15 MPa at 7 and 28 days, respectively, was obtained when mixing and casting under hot weather conditions. It is probably due to increases in precipitation of hemicarboaluminate and monocarboaluminate as a strength-promoting mechanism in limestone fillerized systems (MOON *et al.*, 2017; SCHÖLER *et al.*, 2017), especially when this precipitation is accelerated under the greater mixing and casting temperature by the hot climate due to a thermo-activation of the hydration reactions (SALHI *et al.*, 2020).

In terms of replacement of limestone filler by calcium-rich ashes at  $20 \pm 2$  °C and mixing in hot weather conditions, the compressive strength at 1 and 7 days was improved or at least maintained when 50% of limestone filler was replaced with calcium-rich ashes, compared to the reference mixture. It is believed that this behavior results from the better dispersion of the cement particles, which increases the number of nucleation sites owing to the morphology of the calcium-rich ash compared to that of the limestone filler. This indicates that the presence of calcium-rich ash in the system can accelerate the initial hydration reactions of the cement compounds.

Within the literature, it is noted that in concrete produced in hot climate environments, the compression strength increases at early ages for vibrated concrete (KANSTAD *et al.*, 2003; MOURET; BASCOUL; ESCADEILLAS, 2005; ORTIZ *et al.*, 2005). This fact was also observed in the mixtures corrected with water and, mainly, in the mixtures corrected with superplasticizer, which is justified by the greater compactness of the mixture resulting from the water evaporation. When the ashes were incorporated into the system, a similar behavior was observed.

Regarding the strength at 28 days or more, the literature reports losses in vibrated concrete produced in hot weather environments (BURG, 1996; KIM; HAN; SONG, 2002; KANSTAD *et al.*, 2003; MOURET; BASCOUL; ESCADEILLAS, 2005; ORTIZ *et al.*, 2005). However, Nóbrega *et al.* (2018) did not observe this behavior in SCCs. Likewise, no losses were observed in the SCC compression strengths for TFC (100% of limestone filler), and TFCFA (50% of limestone filler + 50% of calcium-rich ash filler) and their respective corrections when exposed to heat during the mixing process. Nascimento *et al.* (2019) also reported the precipitation of hemicarboaluminate and monocarboaluminate phases in calcium-rich systems using Albaroba ashes.

Table 6 presents the results of the One-Way ANOVA (analysis of variance) applied to study the effects of replacing the limestone filler with the rich-calcium carbonate ashes on the compressive strength at 28 days.

Table 6 - One-Way ANOVA results to compressive strengths at 28 days of curing

Source of variation	Sum of squares	Degrees of freedom	Mean square	F	p-value	F-critical	Significance criteria ( $p < 0.05$ )
<b>TFC - TFCFA - TFA</b>							
Between Treatments	101.48	2	50.74	44.07	2.96E-06	3.89	Significant
Error (or Residual)	13.82	12	1.15				
Total	115.30	14					
<b>TFC-W – TFCFA-W – TFA-W</b>							
Between Treatments	90.21	2	45.10	25.36	4.90E-05	3.89	Significant
Error (or Residual)	21.34	12	1.78				
Total	111.55	14					
<b>TFC-S – TFCFA-S – TFA-S</b>							
Between Treatments	515.77	2	257.89	161.26	2.13E-09	3.89	Significant
Error (or Residual)	19.19	12	1.60				
<b>Total</b>	<b>534.96</b>	<b>14</b>					

The ANOVA results at a confidence level of 95% (0.05 level of significance) suggested that the use of ashes was statistically significant ( $p$ -value  $< 0.05$ ) in SCC mixtures for both systems mixed with dry materials at  $20 \pm 2$  °C (TFC - TFCFA - TFA) and those that used heated dry materials to simulate hot weather conditions ( $80 \pm 2$  °C, TFC-W – TFCFA-W – TFA-W, and TFC-S – TFCFA-S – TFA-S). Regarding the two ways to maintain the self-compacting ability (by adding extra water or overdosing superplasticizer), it can be observed in Table 6 that the effect of using ashes was statistically more significant when the superplasticizer has overdosed, presenting smaller  $p$ -values. Tukey's test showed that the mixtures TFA, TFA-W, and TFA-S presented means that are significantly different ( $p < 0.05$ ) from each other.

It is believed that total replacement by the residue (TFA, 100% of calcium-rich ash filler) interferes in a way that affects hydration at older ages because calcium-rich ash improves the dispersion of cement particles and increases the number of nucleation points, causing loss of strength. However, the substitution of 50% of limestone filler with calcium-rich ashes maintains the values of compression strength at higher ages. When the mixture was corrected using a superplasticizer, the responses improved. However, it is important to highlight that it was not possible to produce a SCC of class SF2 for TFA-S, but its compressive strength was achieved to comparison.

### Water transport properties

The average results of total water absorption, in descending order, were as follows (standard deviation of three samples):  $7.56 \pm 0.05\%$  (TFA-W)  $> 7.12 \pm 0.05\%$  (TFA)  $\cong 7.1 \pm 0.10\%$  (TFCFA-W)  $> 6.7 \pm 0.04\%$  (TFA-S)  $> 6.3 \pm 0.15\%$  (TFC-W)  $> 5.94 \pm 0.16\%$  (TFCFA)  $\cong 5.9 \pm 0.07\%$  (TFC-S)  $> 5.65 \pm 0.15\%$  (TFCFA-S)  $> 4.5 \pm 0.05\%$  (TFC-S). Ratifying the results of compression strength, the correction with water, despite recomposing the water evaporated by the temperature of the materials during mixing and molding of the SCCs, thus ensuring the properties of self-compacting in the fresh state, negatively influenced the microstructural density of the cement system. The increase in the water-cement ratio increases the number of voids, leaving the system less resistant and more permeable.

The One-Way ANOVA's results ( $p$ -value  $< 0.05$ , Table 7) suggested that replacing the limestone filler with ashes statistically influence the water absorption at 28 days for both systems mixed with dry materials at  $20 \pm 2$  °C (TFC - TFCFA - TFA) and those that used heated dry materials ( $80 \pm 2$  °C, TFC-W – TFCFA-W – TFA-W, and TFC-S – TFCFA-S – TFA-S). The effect of using ashes was statistically more significant when the superplasticizer has overdosed, as in the compressive strength. Tukey's test indicated significantly different means ( $p < 0.05$ ) for the ash-incremented mixtures in all conditions.

The correction with superplasticizer addition produced results in the opposite direction, where better compression strength and lower total water absorption were observed for the SCCs that used heated dry materials to simulate hot weather mixing. There was an improvement in the granular arrangement, which

promoted a less permeable system due to the reduction in the water/total fines ratio. The lowest value of total water absorption was found for TFC-S, confirming its greatest result of compression strength.

The capillary absorption results were in line with the compression strength and total absorption tests. As can be seen in Figure 8 (standard deviation of three samples), the average capillary absorption at 72 h, in descending order, was in agreement with the compression strength and total absorption tests.

### Electrical resistivity

The higher the electrical resistivity, the less permeable is the sample, because a denser and more compact microstructure does not provide ionic mobility. The average results of the electrical resistivity (plus standard deviation of three samples) confirmed the behavior of the compression strength and absorption of water. As can be seen in Figure 9, TFA and TFA-W exhibited the lowest electrical resistivities, while TFC-S and TFCFA-S were more resistant to reinforced steel corrosion problems. Furthermore, all SCCs obtained electrical resistivity results higher than 200  $\Omega$  m with an insignificant (MEHTA; MONTEIRO, 2008). Hence, mixing and curing SCC in hot weather conditions (both extra-water and superplasticizer corrections) using or not Algaroba ashes in all evaluated proportions did not affect their probability of corrosion rates.

Table 7 - One-Way ANOVA results to total water absorption at 28 days

Source of variation	Sum of squares	Degrees of freedom	Mean square	F	p-value	F-critical	Significance criteria (p < 0.05)
<i>TFC - TFCFA - TFA</i>							
Between Treatments	2.1464	2	1.0732	111.7917	1.78E-05	5.14	Significant
Error (or Residual)	0.0576	6	0.0096				
Total	2.204	8					
<i>TFC-W – TFCFA-W – TFA-W</i>							
Between Treatments	2.4392	2	1.2196	109.5449	1.89E-05	5.14	Significant
Error (or Residual)	0.0668	6	0.011133				
Total	<b>2.506</b>	<b>8</b>					
<i>TFC-S – TFCFA-S – TFA-S</i>							
Between Treatments	3.345	2	1.6725	168.3725	5.36E-06	5.14	Significant
Error (or Residual)	0.0596	6	0.009933				
Total	<b>3.4046</b>	<b>8</b>					

Figure 8 - Capillary absorption at 72h

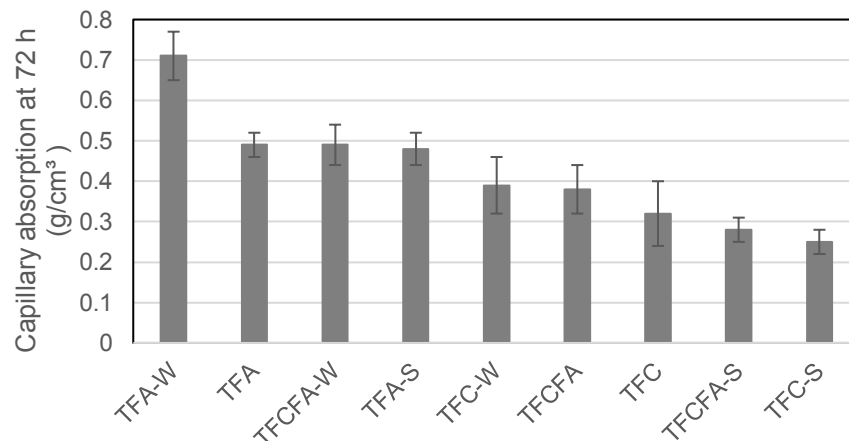
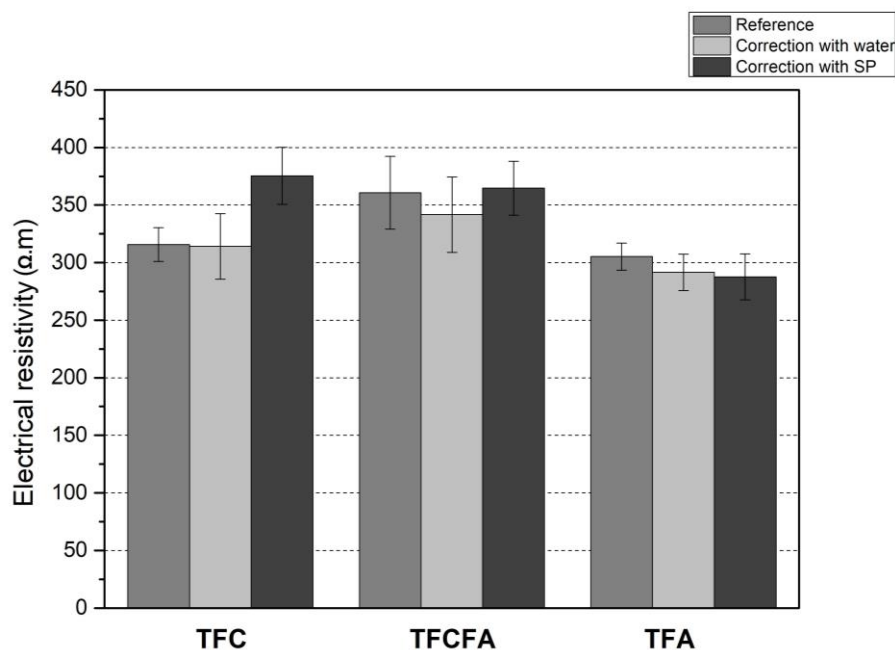


Figure 9 - Electrical resistivity at 28 days



As indicated in Table 8, the ANOVA results ( $p$ -value  $< 0.05$ ) suggested that replacing limestone filler with ashes statistically influence the electrical resistivity at 28 days for both systems mixed with dry materials at  $20 \pm 2$  °C (TFC - TFCFA - TFA) and those corrected using superplasticizer under heated dry materials ( $80 \pm 2$  °C, TFC-S - TFCFA-S - TFA-S). On the other hand, the electrical resistivity was not significantly influenced when the flow ability was corrected using water ( $80 \pm 2$  °C, TFC-W - TFCFA-W - TFA-W). Tukey's test indicated significantly different means ( $p < 0.05$ ) for the TFCFA and TFA-S mixtures.

### Acid attack

The average results found through the acid attack tests (acetic, sulfuric, and hydrochloric) are presented in Figure 10 along with the standard deviation of three samples for each mixture. As it was impossible to produce an SCC of class SF2 for TFA-S, the loss of weight after the acid attack of TFA-W and TFA-S was not evaluated.

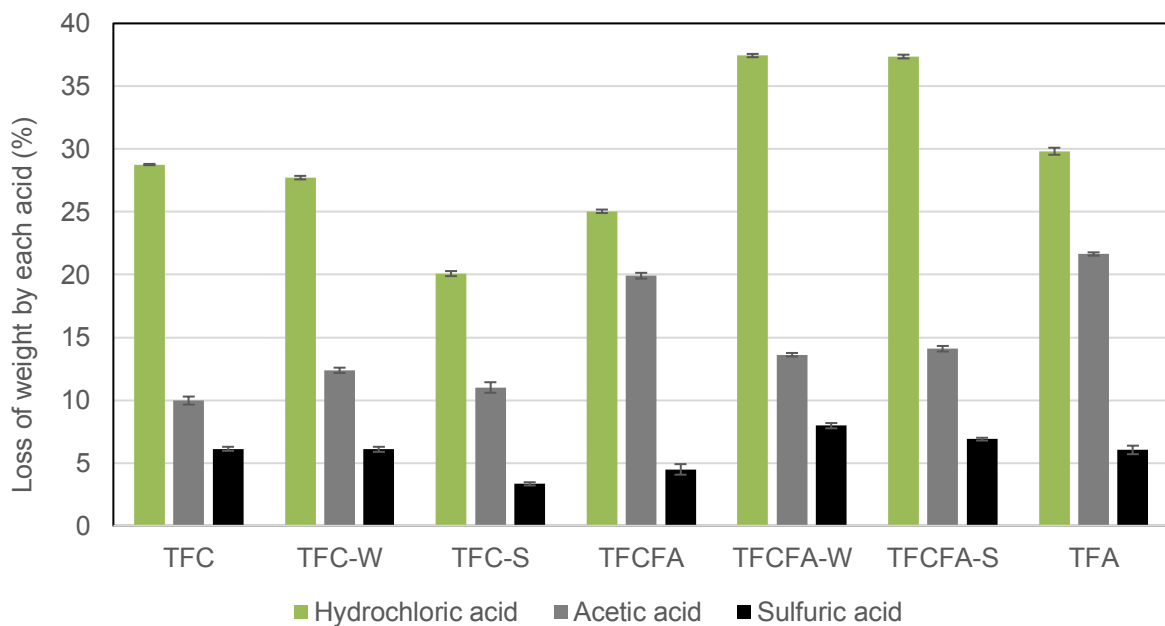
It can be observed that hydrochloric acid is the most aggressive to concrete, with losses of mass close to 38%, whereas sulfuric acid is the least aggressive to concrete, with a maximum loss of approximately 7%. Hydrochloric acid promotes the progressive neutralization of the alkaline nature of the cement matrix through the decomposition of the main hydrated products ( $\text{Ca}(\text{OH})_2$  and C-S-H), forming soluble calcium chloride ( $\text{CaCl}_2$ ) and water (DONATELLO; PALOMO; FERNÁNDEZ-JIMÉNEZ, 2013).

Further, concerning hydrochloric acid, it was observed that TFCFA-W and TFCFA-S obtained the most significant results, indicating that production in hot weather conditions increases the weight loss of concrete when subjected to this type of acid. This phenomenon may be related to the more porous network (greater tendency to water absorption) of the systems mixed and molded under hot weather conditions, and the acid penetration inside it is facilitated. Moreover, the more accelerated precipitation of Portlandite due to the mixing temperature, makes the system richer in calcium, and easily degraded by the hydrochloric acid. Further analyses of the hydration products are necessary to prove this theory. When the pH is reduced to values below 12, calcium hydroxide is dissolved, and it contributes to a connected path of porous capillaries that allows acid ions to penetrate deeper into the internal structure. Further, the decrease in alkalinity caused the disintegration of the hydrated calcium silicate structure and increased pore size (CHATVEERA; LERTWATTANARUK, 2014).

Table 8 - One-Way ANOVA results to electrical resistivity at 28 days

Source of variation	Sum of squares	Degrees of freedom	Mean square	F	p-value	F-critical	Significance criteria (p < 0.05)
<i>TFC – TFCFA – TFA</i>							
Between Treatments	5217.73	2	2608.87	5.78129	0.03987	5.14	Significant
Error (or Residual)	2707.56	6	451.26				
Total	7925.29	8					
<i>TFC-W – TFCFA-W – TFA-W</i>							
Between Treatments	3762.93	2	1881.46	2.66127	0.14881	5.14	Not significant
Error (or Residual)	4241.87	6	706.98				
Total	<b>8004.80</b>	<b>8</b>					
<i>TFC-S – TFCFA-S – TFA-S</i>							
Between Treatments	13731.22	2	6865.21	13.1735	0.00638	5.14	Significant
Error (or Residual)	3127.02	6	521.17				
<b>Total</b>	<b>16858.24</b>	<b>8</b>					

Figure 10 - Loss of weight after the acid attack at 28 days



## Conclusions

Calcium-rich ashes have been proposed as an alternative filler in SCC because they are rich in calcium carbonate. This residue has proved to be a potential source for partial replacement of the limestone filler in SCCs, both under normal temperature and using heated dry materials to simulate hot weather mixing. The following conclusions were drawn from the study:

(a) it was possible to obtain SCCs with the incorporation of calcium-rich ashes (replacement of 50% of the limestone filler) with similar results to those achieved with SCCs produced only with limestone filler both under normal temperature and using heated dry materials to simulate hot weather mixing, maintaining the values of compression strength, permeability, and porosity;

(b) the total substitution of limestone filler with calcium-rich ashes, even for SCC mixed using heated dry materials to simulate hot weather conditions, did not benefit the SCC;

- (c) as calcium-rich ash has a larger specific surface area than the limestone filler, more superplasticizer additives are required for SCC production using 100% of ashes both at  $20 \pm 2$  °C and  $50 \pm 2$  °C; and
- (d) using 50% ash demands less water and superplasticizer when submitted to the simulated hot weather mixing due to a better particle packing.

## References

- AMERICAN CONCRETE INSTITUTE. **ACI 305.1**: specification for hot weather concreting (metric). Farmington Hills, 2014.
- AMERICAN SOCIETY FOR TESTING AND MATERIALS. **C 1260**: standard test method for potential alkali reactivity of aggregates (mortar-bar method). Philadelphia, 2014b.
- AMERICAN SOCIETY FOR TESTING AND MATERIALS. **C 150**: specification for Portland cement. Philadelphia, 2017a.
- AMERICAN SOCIETY FOR TESTING AND MATERIALS. **C 227**: standard test method for potential alkali reactivity of cement-aggregate combinations (mortar-bar method). Philadelphia, 2010.
- ASSOCIAÇÃO BRASILEIRA DE NORMAS TÉCNICAS. **NBR 10005**: procedimento para obtenção de extrato lixiviado de resíduos sólidos. Rio de Janeiro, 2004.
- ASSOCIAÇÃO BRASILEIRA DE NORMAS TÉCNICAS. **NBR 15577-1**: agregados: reatividade álcali-agregado: parte 1: guia para avaliação da reatividade potencial e medidas preventivas para uso de agregados em concreto. Rio de Janeiro, 2018b.
- ASSOCIAÇÃO BRASILEIRA DE NORMAS TÉCNICAS. **NBR 15577-4**: agregados: reatividade álcali-agregado: parte 4: determinação da expansão em barras de argamassa pelo método acelerado. Rio de Janeiro, 2018a.
- ASSOCIAÇÃO BRASILEIRA DE NORMAS TÉCNICAS. **NBR 15823-1**: concreto autoadensável: parte 1: classificação, controle e recebimento no estado fresco. Rio de Janeiro, 2017a.
- ASSOCIAÇÃO BRASILEIRA DE NORMAS TÉCNICAS. **NBR 15823-2**: concreto autoadensável: parte 2: determinação do espalhamento, do tempo de escoamento e do índice de estabilidade visual: método do cone de Abrams. Rio de Janeiro, 2017b.
- ASSOCIAÇÃO BRASILEIRA DE NORMAS TÉCNICAS. **NBR 15823-3**: concreto autoadensável: parte 3: determinação da habilidade passante: método do anel J. Rio de Janeiro, 2017e.
- ASSOCIAÇÃO BRASILEIRA DE NORMAS TÉCNICAS. **NBR 15823-4**: concreto autoadensável: parte 4: determinação da habilidade passante: métodos da caixa I e da caixa U. Rio de Janeiro, 2017c.
- ASSOCIAÇÃO BRASILEIRA DE NORMAS TÉCNICAS. **NBR 15823-5**: concreto autoadensável: parte 5: determinação da viscosidade: método do funil V. Rio de Janeiro, 2017d.
- ASSOCIAÇÃO BRASILEIRA DE NORMAS TÉCNICAS. **NBR 5738**: concreto: procedimento para moldagem e cura de corpos de prova. Rio de Janeiro, 2015.
- ASSOCIAÇÃO BRASILEIRA DE NORMAS TÉCNICAS. **NBR 5739**: concreto: ensaios de compressão de corpos-de-prova cilíndricos. Rio de Janeiro, 2018c.
- ASSOCIAÇÃO BRASILEIRA DE NORMAS TÉCNICAS. **NBR 9778**: argamassa e concreto endurecidos: determinação da absorção de água, índice de vazios e massa específica. Rio de Janeiro, 2009.
- ASSOCIAÇÃO BRASILEIRA DE NORMAS TÉCNICAS. **NBR 9779**: argamassa e concreto endurecidos: determinação da absorção de água por capilaridade. Rio de Janeiro, 2012.
- BRADU, A.; FLOREA, N. Workability and compressive strength of self-compacting concrete containing different levels of limestone powder. **Bulletin of the Transylvania University of Brasov**, v. 8, n. 57, special issue, 2015.
- BURG, R. G. **The influence of casting and curing temperature on the properties of fresh and hardened concrete**. Skokie: Portland Cement Association, 1996.
- CANADIAN STANDARDS ASSOCIATION. **A23.2-25A**: test method for detection of alkali-silica reactive aggregate by accelerated expansion of mortar bars. Mississauga, 2014.

- CHATVEERA, B.; LERTWATTANARUK, P. Evaluation of nitric and acetic acid resistance of cement mortars containing high-volume black rice husk ash. **Journal of Environmental Management**, v. 133, 365–373, 2014.
- DONATELLO, S.; PALOMO, A.; FERNÁNDEZ-JIMÉNEZ, A. Durability of very high volume fly ash cement pastes and mortars in aggressive solutions. **Cement and Concrete Composites**, v. 38, 12–20, 2013.
- GHAFOORI, N.; DIAWARA, H.; HASNAT, A. Remediation of loss in flow properties of self-consolidating concrete under various combinations of transportation time and temperature. **Construction and Building Materials**, v. 192, p. 508-514, 2018.
- HAMPTON, J. S. Extended workability of concrete containing high-range water-reducing admixtures in hot weather. In: MALHOTRA, V. M. **Developments in the use of superplasticizers**. Detroit: American Concrete Institute, 1981.
- KANSTAD, T. *et al.* Mechanical properties of young concrete: part I: experimental results related to test methods and temperature effects. **Materials and Structures**, v. 36, n. 4, p. 218-225, May 2003.
- KIM, J.-K.; HAN, S. H.; SONG, Y. C. Effect of temperature and aging on the mechanical properties of concrete: part I: experimental results. **Cement and Concrete Research**, v. 32, n. 7, p. 1087-1094, Jul. 2002.
- LAVAGNA, L. *et al.* Cement-based composites containing functionalized carbon fibers. **Cement and Concrete Composites**, v. 88, p. 165-171, 2018.
- LELOUP, W. D. A. **Efeito da adição de lodo têxtil e cinzas de lenha gerados no apl de confecções pernambucano em argamassa de cimento Portland**. Caruaru, 2013. 108 f. Dissertação (Mestrado em Engenharia Civil e Ambiental) – Universidade Federal de Pernambuco, Caruaru, 2013.
- LIMA, R. A. P.; MARINHO, E. P.; NÓBREGA, A. C. V. Self-compacting concretes using calcium-rich ashes as alternative fillers. In: INTERNATIONAL CONFERENCE ON NON-CONVENTIONAL MATERIALS AND TECHNOLOGIES, 18., Nairobi, 2019. **Proceedings [...]** Nairobi, 2019.
- MASSARWEH, O. *et al.* Development of a concrete set retarder utilizing electric arc furnace dust. **Construction and Building Materials**, v. 55, p. 119378, 2020.
- MEHTA, P. K.; MONTEIRO, P. J. M. **Concreto: microestrutura, propriedades e materiais**. São Paulo: Ibracon, 2008.
- MELO, M. C. S. D. **Estudo de argamassas adicionadas de cinzas de algaroba geradas no arranjo produtivo local de confecções do agreste pernambucano**. Caruaru, 2012. Dissertação (Mestrado em Engenharia Civil e Ambiental) – Universidade Federal de Pernambuco, Caruaru, 2012.
- MELO, M. *et al.* Cal produzida a partir de cinza de biomassa rica em cálcio. **Cerâmica**, v. 64, p. 318–324, 2018.
- MOON, G. D. *et al.* Effects of the fineness of limestone powder and cement on the hydration and strength development of PLC concrete. **Construction and Building Materials**, v. 135, p. 129-136, 2017.
- MOTA, M. H. A. **Concreto seco com incorporação de cinzas de madeira de Algaroba (propositis juliflora) moldado sob pressão**. Caruaru, 2014. Dissertação (Mestrado em Engenharia Civil e Ambiental) – Universidade Federal de Pernambuco, Caruaru, 2014.
- MOURA, L. S. D. **Incorporação de cinzas de algaroba geradas no APL de confecções do agreste Pernambucano em concreto betuminoso usinado a quente – CBUQ**. Caruaru, 2017. Dissertação (Mestrado em Engenharia Civil e Ambiental) – Universidade Federal de Pernambuco, Caruaru, 2017.
- MOURA, L. S. *et al.* Use of calcium-rich wood biomass combustion ashes as filler in hot mix asphalt. **Road Materials and Pavement Design**, v. 23, p. 1-19, 2021.
- MOURET, M.; BASCOUL, A.; ESCADEILLAS, G. Strength impairment of concrete mixed in hot weather: relation to porosity of bulk fresh concrete paste and maturity. **Magazine of Concrete Research**, v. 55, n. 3, p. 215-223, 2003.
- MOURET, M.; BASCOUL, A.; ESCADEILLAS, G. Strength impairment of concrete mixed in hot weather: analysis in relation to physical and chemical properties of hardened concrete. **Magazine of Concrete Research**, v. 57, n. 5, p. 301-308, jun. 2005.
- NASCIMENTO, J. E. M. F. D. **Avaliação dos efeitos da substituição da cal hidratada por cinzas de Algaroba em argamassas de revestimento**. Caruaru, 2014. Dissertação (Mestrado em Engenharia Civil e Ambiental) – Universidade Federal de Pernambuco, Caruaru, 2014.

- NASCIMENTO, J. E. M. F. D. *et al.* Cinza de biomassa rica em calcário como material carbonático em sistemas cimentícios de base Portland. **Cerâmica**, v. 65, p. 85–91, 2019.
- NÓBREGA, A. C. V. *et al.* Improved 28-day compressive strength of SCC mixed and cured in hot. **Construction and Building Materials**, v. 173, p. 650-661, 2018.
- ORTIZ, J. *et al.* Influence of environmental temperatures on the concrete compressive strength: Simulation of hot and cold weather conditions. **Cement and Concrete Research**, v. 35, n. 10, p. 1970-1979, out. 2005.
- PINEAUD, A. *et al.* Mechanical properties of high performance self-compacting concretes at room and high temperature. **Construction and Building Materials**, v. 112, p. 747-755, mar. 2016.
- RAHAL, K. N.; HASSAN, W. Shear strength of plain concrete made of recycled low-strength concrete aggregates and natural aggregates. **Construction and Building Materials**, v. 311, p. 125317, 2021.
- SALHI, M. *et al.* Combined effect of temperature and time on the flow properties of self-compacting concrete. **Construction and Building Materials**, v. 240, p. 117914, 2020.
- SCHÖLER, A. *et al.* Early hydration of SCM-blended Portland cements: a pore solution and isothermal calorimetry study. **Cement and Concrete Research**, v. 93, p. 71-82, 2017.
- TUTIKIAN, B. F.; DAL MOLIN, D. C. **Concreto auto-adensável**. São Paulo: Pini, 2008.
- ZHANG, X.; LI, J. H.; LI, X. F. Influence of slag powder on the water reducing effect of admixtures and its mechanism. **Concrete**, v. 6, p. 34-36, 1999.

## Acknowledgments

Support from CAPES Brazilian Funding (Finance Code 001) and FACEPE (Science and Technology Foundation of the State of Pernambuco, Brazil), through the Academic Research Fund (grant to Mario T. Kato, process number APQ 627 0603-3.07/14, IBPG-0780-3.01/16), is acknowledged and appreciated.

### Jonatércio Florencio de Vasconcelos Marinho

Investigation. Methodology. Writing - original Draft. Writing - review & editing. Formal analysis. Data curation.

Núcleo de Tecnologia | Universidade Federal de Pernambuco | Av. Marielle Franco, s/n, Km 59, Nova Caruaru | Caruaru - PE - Brasil | CEP 55014-900 | Tel.: (81) 2103-9169 | E-mail: jonatercio.florencio@ufpe.br

### Rodrigo Araújo Pereira Lima

Investigation. Methodology. Writing - review and editing. Formal analysis.

Núcleo de Tecnologia | Universidade Federal de Pernambuco | E-mail: rodrigo.araujolima@ufpe.br

### Erika Pinto Marinho

Supervision. Validation. Writing - review and editing.

Núcleo de Tecnologia | Universidade Federal de Pernambuco | E-mail: erika.pmarinho@ufpe.br

### Ana Cecília Vieira da Nóbrega

Conceptualization. Formal analysis. Funding acquisition. Project Administration. Supervision. Validation. Writing - review and editing.

Departamento de Engenharia Civil e Ambiental | Universidade Federal do Rio Grande do Norte | Caixa Postal 1524 | Campus Universitário Lagoa Nova | Natal - RN - Brasil | CEP 59078-900 | Tel.: (84) 3215-3723 | E-mail: anacecilia.nobrega@ufpe.br

## Ambiente Construído

Revista da Associação Nacional de Tecnologia do Ambiente Construído  
Av. Osvaldo Aranha, 99 - 3º andar, Centro  
Porto Alegre - RS - Brasil  
CEP 90035-190  
Telefone: +55 (51) 3308-4084  
www.seer.ufrgs.br/ambienteconstruido  
www.scielo.br/ac  
E-mail: ambienteconstruido@ufrgs.br



This is an open-access article distributed under the terms of the Creative Commons Attribution License.